Hindawi
Advances in Materials Science and Engineering
Volume 2018, Article ID 8560604, 11 pages
https://doi.org/10.1155/2018/8560604

Research Article

Material Composition Design and Anticracking Performance Evaluation of Asphalt Rubber Stress-Absorbing Membrane Interlayer (AR-SAMI)

Ke Zhang,[1,2] Zhengqi Zhang,[2] and Yaofei Luo[2]

[1]*College of Information Engineering, Fuyang Normal University, Fuyang, Anhui 236041, China*
[2]*Key Laboratory for Special Area Highway Engineering of Ministry of Education, Chang'an University, Xi'an, Shaanxi 710064, China*

Correspondence should be addressed to Zhengqi Zhang; z_zhengqi@126.com

Received 24 April 2018; Accepted 19 June 2018; Published 30 July 2018

Academic Editor: Paolo Andrea Carraro

To promote the application of the asphalt rubber stress-absorbing membrane interlayer (AR-SAMI), the material composition design and the evaluation of antireflective cracking effect of AR-SAMI need to be studied. In this paper, conventional asphalt tests, dynamic shear rheometer (DSR) test, and fatigue cracking test were conducted to evaluate the high and low temperature performance, elastic recovery property, and antifatigue performance of SK90# raw asphalt, asphalt rubber, and SBS-modified asphalt. The AR-SAMI's material composition design method based on the interlaminar shear strength was put forward. The influence of the asphalt application rate and aggregate application rate on interlaminar shear strength was also discussed to determine the optimum material composition. The fatigue cracking test was designed based on the Hamburg rutting instrument, and the cracking resistance of AR-SAMI was analyzed. The results indicate that asphalt rubber is the suitable binder for SAMI. The application rates of asphalt and aggregate have significant impact on the interlaminar shear strength of AR-SAMI. The optimum binder application rate of asphalt rubber and aggregate application rate are 2.2 kg/m^2 and 14 kg/m^2, respectively, for AR-SAMI. The fatigue cracking life and fatigue fracture life of composite specimens increase obviously after AR-SAMI is paved. The increasing range of fatigue life because of the use of AR-SAMI is up to 30% under the dry condition of 15°C. The decreasing range of fatigue life caused by water reaches as high as 50%. The fatigue life falls sharply when the temperature increases from 15°C–25°C to 35°C–45°C.

1. Introduction

Large amounts of cement concrete pavements were built in China from the early 1970s to the late 1980s. These pavements are just in the period of large- and medium-sized maintenance [1]. Among the measures which are employed to deal with the old cement concrete pavement, the paving asphalt layer is one of the most common treatment methods [2]. Asphalt overlays can not only improve the performance of cement concrete pavements but also make full use of the residual strength of the old cement concrete slabs. Meanwhile, the construction of asphalt overlays has little influence on the traffic and environment [3, 4]. However, there are also some problems about asphalt overlays needed to be solved. The asphalt overlay is likely to generate reflective cracks under the cyclic traffic loading due to the existing joints and cracks in the old cement concrete slab, and the reflective cracks usually propagate to the asphalt surface in a short time [5–7]. Additionally, the reflective cracks will cause the degradation of pavement performance and affect the appearance of asphalt overlays. The cracks also provide access to road-surface water to infiltrate into the pavement and affect the strength of subgrade, thus causing the reduction of stability and overall strength of pavement [8, 9].

To solve the problem of reflective cracks in asphalt overlays paved on the rigid or semirigid pavement, many road engineers carried out lots of researches. Noori et al. [10] demonstrated that STRATA had a significant performance

Table 1: Technical indexes of SK90# raw asphalt.

Items		Measured value	Specification limits	Cited specifications
Penetration (25°C, 100 g, 5 s, 0.1 mm)		91	80~100	ASTM D5-97
Penetration index (PI)		−0.2985	−1.0~+1.0	—
Ductility (10°C, 5 mm/min, cm)		>100	≥45	ASTM D113-99
Softening point (°C)		48.9	≥45	ASTM D36-06
Specific gravity		0.979	—	ASTM D70-76
RTFO treated at 163°C for 85 min	Mass loss (%)	−0.34	≤±0.8	ASTM D2872-04
	Residual penetration ratio (25°C, %)	72.9	≥57	ASTM D5-97
	Residual ductility (10°C, cm)	15	≥8	ASTM D113-99

advantage in retarding the propagation of reflective cracks. Norambuena-Contreras and Gonzalez-Torre [11] studied the influence of different geosynthetics on retarding the reflective cracks of asphalt overlays. It was found that the good tensile behavior of geosynthetic cannot assure the function of delaying the propagation of reflective cracks. Kim and Buttlar [12] found that the base-isolating interlayer between asphalt overlays and old concrete slabs can improve the stress state in asphalt overlays. Ogundipe et al. [13, 14] carried out researches on the performance of the stress-absorbing membrane interlayer (SAMI) under traffic loading. The results indicated that the SAMI can effectively delay the generation and propagation of reflective cracks. Tan et al. [15] evaluated the performance of the high viscous stress-absorbing layer by routine laboratory tests and found that the viscous asphalt stress-absorbing layer has an excellent ability to prevent the reflective cracks.

The previous studies show that the stress-absorbing membrane interlayer (SAMI) can not only solve the existing problems of reflective cracks in asphalt overlays but also extend the service life of the composite pavement. In addition, it can reduce the cost of repair and maintenance for pavement, thus decreasing the life-cycle costs of the pavement. However, the studies of SAMI are mostly about its effect on retarding reflective cracks in asphalt overlays but rarely involve the material composition design. Meanwhile, most of the instruments used in previous studies belong to conventional test equipment, which is difficult to obtain the actual conclusions.

In addition, the number of waste tires increased with the development of automobile industries quickly. Waste tires belong to a kind of industrial solid waste which will threaten human health and cause irreversible damage to the environment [16]. From the environmental perspective, the waste tires must be utilized [17]. One widely used recycling approach for waste tires is to break down the tires to produce rubber powder [18]. Rubber powder is the most widely used polymer modifier for raw asphalt [19, 20]. If the asphalt rubber can be utilized in SAMI, the environmental pollution caused by waste tires can be greatly reduced. Therefore, the problems about material composition design and the reflective cracking resistance of AR-SAMI need to be studied systematically.

In this paper, firstly, the conventional asphalt tests, DSR test, and fatigue cracking test of different asphalt binders were conducted to select the appropriate asphalt for SAMI. Then, the composite specimens with and without AR-SAMI were shaped at different application rates of asphalt and aggregate. The interlaminar shear tests at 25°C and 45°C were carried out to determine the optimum asphalt application rate and aggregate application rate of AR-SAMI. Finally, the wheel loading of the Hamburg rutting instrument was selected to simulate the effect of vehicles on the road. Based on the Hamburg rutting test, the fatigue cracking tests were carried out under different conditions, and the fatigue cracking life and fatigue fracture life were monitored to evaluate the influence of AR-SAMI in retarding the reflective cracks.

2. Materials and Methods

2.1. Materials

2.1.1. Raw Asphalt, Asphalt Rubber, and SBS-Modified Asphalt. The raw asphalt used in this paper was SK90#. The main technical indexes of the raw asphalt are listed in Table 1. The asphalt rubber was prepared by SK90# raw asphalt and the rubber powder of 40 mesh in the laboratory, and the mixing amount of rubber powder accounted for 19% by raw asphalt weight. The main technical indexes of rubber powder are listed in Table 2. The SBS-modified asphalt was also prepared by SK90# raw asphalt and SBS modifier in the laboratory, and the mixing amount of the SBS modifier was 4%.

2.1.2. Aggregate. The coarse and fine aggregates are basalt aggregates, and the mineral powder is limestone powder. Various technical indexes of aggregates and mineral powder are listed in Tables 3 and 4, which can meet the requirements of Chinese current standards.

According to the international experience, the aggregate of single particle size is usually applied in the AR-SAMI. In this research, the aggregate of single particle size of 9.5–13.2 mm is used. The gradation of SMA-13 is listed in Table 5.

2.2. Test Method

2.2.1. Conventional Asphalt Tests. The cracking resistance of SAMI is mainly dependent on the performance of the asphalt binder. The conventional indexes such as penetration, softening point, ductility, elastic recovery, and viscosity can reflect the properties of asphalt from different aspects.

Table 2: Main technical indexes of rubber powder.

Items	Measured value	Specification limits	Cited specifications
Relative density	1.19	1.10~1.30	
Water content (%)	0.48	<1	
Metal content (%)	0.023	<0.05	
Fiber content (%)	0.45	<1	JT/T 798-2011
Ash content (%)	3.9	≤8	
Acetone extracts (%)	14	≤22	
Carbon black content (%)	43	≥28	

Table 3: Technical indexes of basalt aggregates.

Item	Technical index (%)	Test results	Test method
Crushing value	≤15	11	T0316
Los Angeles abrasion loss	≤28	15.1	T0317
Sturdiness	≤12	11.8	T0314
<0.075 mm grain content	≤1	0.41	T0310
Apparent relative density (g·cm^{-3})	⩽2.5	2.719	T0304
Water absorption (%)	0.553	⩾2.0	T0304

Table 4: Technical indexes of mineral powder.

Item	Unit	Test results	Index value
Apparent density	—	2.825	≥2.5
Hydrophilic coefficient	—	0.73	<1
Plasticity index	%	3.5	<4
Water content	%	0.1	≤1
Mesh size <0.6 mm	%	100	100
Mesh size <0.15 mm	%	95.4	90–100

The penetration (25°C), softening point, ductility (5°C), and elastic recovery of raw asphalt, rubber asphalt, and SBS-modified asphalt were measured in accordance with the standards of ASTM D5, ASTM D36, ASTM D6084, and ASTM D113, respectively. The viscosity of the three kinds of asphalt was tested by a Brookfield rotational viscometer (model DV-II+) at 135°C and 177°C according to the standard ASTM D4402.

2.2.2. Interlaminar Shear Test. The C30 concrete slab of 5 cm thickness was prepared, and then, the AR-SAMI containing different application rates of asphalt and aggregate was overlaid on the concrete slab, as shown in Figure 1. The composite slabs were formed after the 5 cm SMA asphalt mixture was paved upon the SAMI. Then, the core samples were drilled from the composite slabs by a core machine. The diameter of the core sample was 100 mm, as shown in Figure 2. The number of replicates for the interlaminar shear test was three. The shear strength of the core sample was tested by the interlaminar shear instrument and can be calculated by the following equation [21]:

$$\tau = \frac{F}{S}, \quad (1)$$

where τ is the interlaminar shear strength (MPa), F is the applied load (N), and S is the bond area (m^2) (here, 7.85×10^{-3} m^2).

The interlaminar shear test was carried out at 25°C (room temperature) and 45°C (high temperature) according to the actual climate condition of Xi'an. And the interlaminar shear tests were conducted at asphalt application rates of 1.8, 2.0, 2.2, 2.4, and 2.6 kg/m^2. At each asphalt application rate, the samples were prepared and tested at five aggregate application rates of 10, 12, 14, 16, and 18 kg/m^2. The test results were also analyzed to determine the influence of the asphalt application rate and aggregate application rate on the shear strength of AR-SAMI.

2.2.3. Fatigue Cracking Test. The composite beam specimen consisted of the C30 concrete slab, AR-SAMI, and asphalt layer. The thickness of the asphalt layer was 50 mm, the thickness of AR-SAMI was 15 mm, and the concrete slab thickness was 50 mm. The length and width of the beam specimen were 500 mm and 100 mm, respectively. A 10 mm notch was sawn at the centre of the slab through the cement concrete layer to simulate the existing cracks of the old pavement [14]. The test loading model and composite beam specimen of the fatigue cracking test are shown in Figure 3. To observe the generation and propagation of reflective cracks clearly, both sides of the asphalt layer and AR-SAMI were painted as white.

The wheel of the Hamburg rutting instrument was selected as a loading device to load on the composite specimen. The number of replicates for the fatigue cracking test was three. The effect of vehicles on the pavement was simulated by the backward and forward loading of wheels on the test specimen. The wheel loading of the Hamburg rutting instrument is 0.7 MPa, and the loading frequency is 52 times/min.

The fatigue cracking resistance of the asphalt mixture is closely related to the environment temperature. The fatigue damages of the asphalt mixture usually occur between 13°C and 15°C, corresponding to the temperature in the spring and rainy seasons of northern China. 15°C is the temperature condition of allowable tensile stress in the specifications for design of asphalt pavement [22]. Therefore, the test

Table 5: The gradation of SMA-13.

Mesh size (mm)	16.0	13.2	9.5	4.75	2.36	1.18	0.6	0.3	0.15	0.075
Passing ration (%)	100.0	95.4	61.3	25.0	19.4	18.4	16.5	13.4	12.6	9.0

Figure 1: The laying of SAMI on the concrete slab.

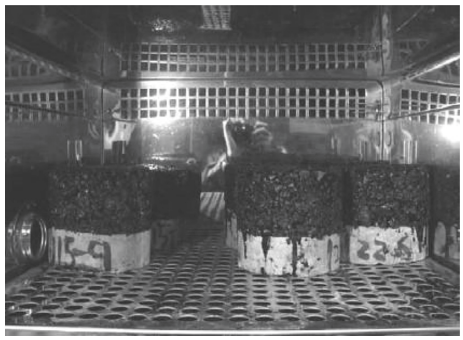

Figure 2: The specimen of the interlaminar shear test.

temperature for the fatigue cracking test is 15°C. At the same time, in order to analyze the influence of moisture and temperature on the fatigue cracking resistance of AR-SAMI, the fatigue cracking tests were carried out in a water bath environment at 15°C, 25°C, 35°C, and 45°C, respectively.

The evaluation indexes of the fatigue cracking test are fatigue cracking life and fatigue fracture life. The fatigue cracking life is defined as the loading times of the Hamburg rut instrument corresponding to the generation of reflective cracks in the asphalt layer. The fatigue fracture life is defined as the loading times corresponding to the reflective crack propagation to the top surface of the asphalt layer [23]. It is thought that the reflective cracking resistance of the composite specimen is better if the fatigue cracking or fracture life is longer.

In this paper, the fatigue cracking tests of composite specimens with and without AR-SAMI under different conditions were carried out. The process of the fatigue cracking test is shown in Figure 4. The test conditions and programs are listed in Table 6.

During the test process, the camera Nikon D7000 was used to record the generation and propagation of reflective cracks. Before the test, appropriate resolution of the camera should be set. The selected resolution meets the requirements for reflective crack identification. So after the test, the compaction time of the fatigue cracking test corresponding to the cracking or fracture of composite specimens can be accurately determined by observing videos. Then, the fatigue cracking life and fatigue fracture life of composite specimens can be obtained by multiplying rolling time with the loading action frequency of 52 times/min, as shown in the following equations:

$$N_C = t_C \times R, \tag{2}$$

where N_C is the fatigue cracking life, t_C is the rolling times of the test wheel corresponding to the cracking (min), and R is the loading action frequency (m^2) (here, 52 times/min).

$$N_F = t_F \times R, \tag{3}$$

where N_F is the fatigue fracture life, t_F is the rolling times of the test wheel corresponding to the fracture (min), and R is the loading action frequency (m^2) (here, 52 times/min).

3. Results and Discussion

3.1. The Optimization of Asphalt Binder for SAMI

3.1.1. Conventional Asphalt Tests. The conventional tests of raw asphalt, SBS-modified asphalt, and asphalt rubber were carried out, and the test results are listed in Table 7.

It can be seen from Table 7 that the penetrations of raw asphalt, SBS-modified asphalt, and asphalt rubber increase with different scales as the temperature rises. Compared with other two kinds of asphalt, the penetration of asphalt rubber at different temperatures is the smallest. The PI value of asphalt rubber is the biggest, indicating that the temperature sensitivity of asphalt rubber is the best. The softening point of asphalt rubber is 68.5°C, which is higher than that of raw asphalt by 40.1% and approaches to that of SBS-modified asphalt. The change of penetration and softening point implies that the mixing of rubber powder can improve the high temperature performance of raw asphalt.

The ductility can be used to characterize the low-temperature deformation resistance of asphalt. High low-temperature ductility indicates that the asphalt is not easy to brittle fracture. The order of ductility is SBS-modified asphalt > asphalt rubber > SK90# raw asphalt. The low-temperature ductility of asphalt rubber increases after the full swelling of rubber powder in raw asphalt at high temperature; namely, the low temperature performance of raw asphalt to resist embrittlement is improved.

The elastic recovery rate of asphalt binder at 25°C reflects the displacement restoring capacity of asphalt pavement. The higher the elastic recovery rate, the stronger the displacement restoring capacity of asphalt pavement; namely, asphalt pavement has the better fatigue resistance. The data of the elastic recovery test at 25°C in Table 5 indicate that SBS-modified asphalt and asphalt rubber have good resilience, which can greatly improve the antifatigue performance of asphalt and extend the fatigue life of the pavement.

At 135°C and 177°C, the viscosity order is asphalt rubber > SBS-modified asphalt > SK90# raw asphalt.

Figure 3: The loading model (a) and beam specimen (b) of the fatigue cracking test.

The viscosity of asphalt rubber at 177°C is 3.097 Pa·s, which can also meet the design requirements of binder viscosity (1.5 Pa·s~4.4 Pa·s). On the whole, the asphalt rubber has excellent cohesiveness.

3.1.2. DSR Test. The complex module (G^*) and phase angle (δ) of asphalt rubber, SBS-modified asphalt, and SK90# raw asphalt are shown in Figures 5 and 6.

As shown in Figure 5, the G^* of the three kinds of asphalt has good linear correlations with temperatures in the semilogarithmic coordinate. The G^* values of the three kinds of asphalt decrease with the increasing temperatures and then reach roughly equal at 40°C. The change ratio of raw asphalt is the fastest, followed by SBS-modified asphalt, and the lowest change ratio belongs to asphalt rubber. Figure 6 shows that the δ of asphalt increases gradually with the increasing temperatures. When the temperature is below 25°C, the δ of SBS-modified asphalt is approximately equal to that of raw asphalt. But the δ of SBS-modified asphalt is less than that of raw asphalt when the temperature is higher than 25°C. As for asphalt rubber, the δ remains at a low level with the change in temperature. Clearly, asphalt rubber has lower temperature sensitivity when compared with raw asphalt and SBS-modified asphalt.

The $G^*\cdot\sin\delta$ of raw asphalt, SBS-modified asphalt, and asphalt rubber at different temperatures is shown in Figure 7.

In Figure 7, the fatigue factor ($G^*\cdot\sin\delta$) of the three kinds of asphalt also has good linear correlations with temperatures in the semilogarithmic coordinate. The $G^*\cdot\sin\delta$ falls gradually with the rise of temperature, which indicates the fatigue resistance of asphalt binder increases gradually. The $G^*\cdot\sin\delta$ of raw asphalt is greater than 5000 kPa at 16°C, exceeding the fatigue limit of Superpave PG specification. The $G^*\cdot\sin\delta$ of SBS-modified asphalt is also greater than 5000 kPa at 13°C, but that of asphalt rubber still remains below 4000 kPa at 13°C. Obviously, the fatigue resistance of asphalt rubber is the best among the three kinds of asphalt, followed by SBS-modified asphalt, and that of raw asphalt is the worst.

3.1.3. Fatigue Cracking Test. The fatigue cracking tests of composite beam specimens with SAMI containing SK90# raw asphalt, SBS-modified asphalt, and asphalt rubber were carried out under the dry condition of 15°C. The asphalt spraying content of the three kinds of composite beam specimens is 2.2 kg/m^2, and the gravel spreading amount is 14 kg/m^2. The influence of asphalt type on fatigue cracking life and fatigue fracture life is shown in Figure 8.

Figure 4: The process of the fatigue cracking test.

Table 6: The test conditions and programs of the fatigue cracking test.

Test conditions	Overlay types	Asphalt application rate (kg/m^2)		Aggregate application rate (kg/m^2)
Dry (15°C)	With SAMI	SK90# raw asphalt	2.2	14.0
		SBS-modified asphalt		
		Asphalt rubber		
	No AR-SAMI	—		—
	With AR-SAMI	1.6		14.0
		1.9		14.0
		2.2		14.0
		2.5		14.0
Water bath (15°C, 25°C, 35°C, and 45°C)	No AR-SAMI	—		—
	With AR-SAMI	1.6		14.0
		1.9		14.0
		2.2		14.0
		2.5		14.0

It can be seen from Figure 8 that the fatigue cracking life and fatigue fracture life of composite beam specimens with SK90# and SAMI is the minimum, followed by SBS-modified asphalt, and the life of composite beam specimens with AR-SAMI is the maximum, which indicates the fatigue

Table 7: Conventional properties of asphalt.

Test items	Units	Test results		
		Raw asphalt	Asphalt rubber	SBS-modified asphalt
Penetration (15°C)	0.1 mm	32	23	29
Penetration (25°C)	0.1 mm	91	50	71
Penetration (30°C)	0.1 mm	140	78	110
PI	—	−0.2985	0.7330	0.2557
Softening point	°C	48.9	68.5	72.3
Ductility (5°C)	cm	6.4	17	29
Elastic recovery (25°C)	%	7.17	75.5	90.3
Viscosity (135°C)	Pa·s	0.327	3.3	1.968
Viscosity (177°C)	Pa·s	—	3.097	0.298

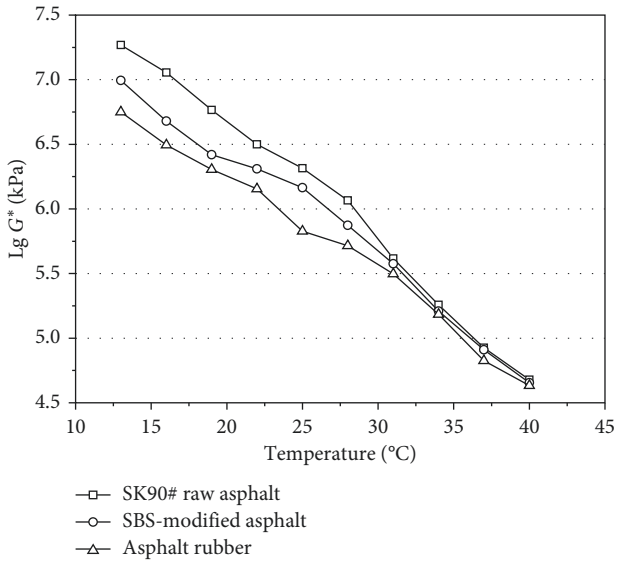

Figure 5: Lg G^* of asphalt at different temperatures.

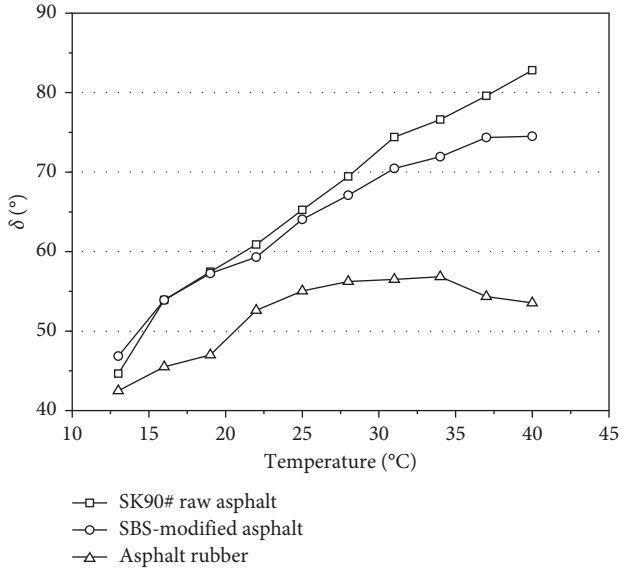

Figure 6: Phase angles of asphalt at different temperatures.

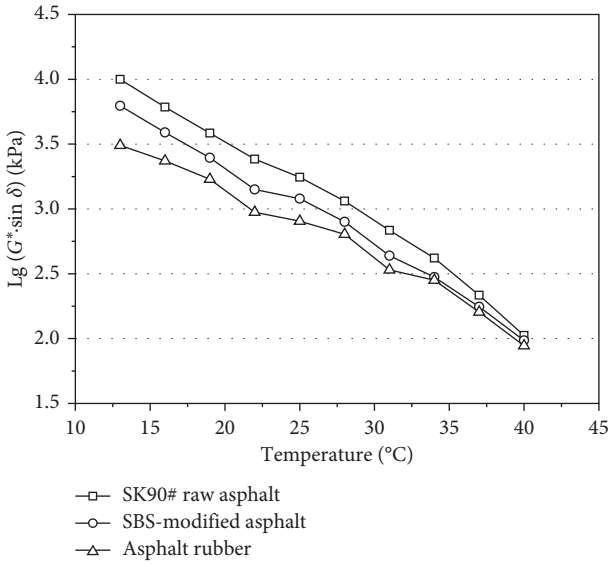

Figure 7: Lg (G^*·sin δ) of asphalt at different temperatures.

property of composite beam specimens with AR-SAMI is the best. Based on the above studies, the asphalt rubber has excellent high and low temperature performance, elastic recovery property, and fatigue resistance. High elasticity and antifatigue properties of asphalt rubber can well meet the functional requirements of SAMI. Therefore, the asphalt rubber is recommended as the binder for SAMI when the asphalt layer is paved on the old cement concrete pavement.

3.2. Material Composition Design of AR-SAMI

3.2.1. Material Composition Design Method for AR-SAMI. The AR-SAMI can delay the propagation of cracks from the bottom layer and prevent water infiltrating from the surface when the interlayer bonding is good. However, the beneficial effect of AR-SAMI cannot be achieved if the shear strength between the layers is poor. The interlaminar shear test can qualify the interlayer bonding between the overlay and concrete slab. The greater the shear strength value, the better the bonding between layers. Zhou et al. [24] found that as the shear strength increases, the stress concentration at the crack tip decreases. Therefore, the asphalt and aggregate application rates of AR-SAMI can be determined based on the interlaminar shear strength. The application rates are determined based on the following criteria:

(1) Proper aggregate embedment into asphalt: The proper and reasonable application rates of asphalt and aggregate should not only make the aggregate be well stabilized but also avoid the AR-SAMI forming a weak interlayer in the composite structure.

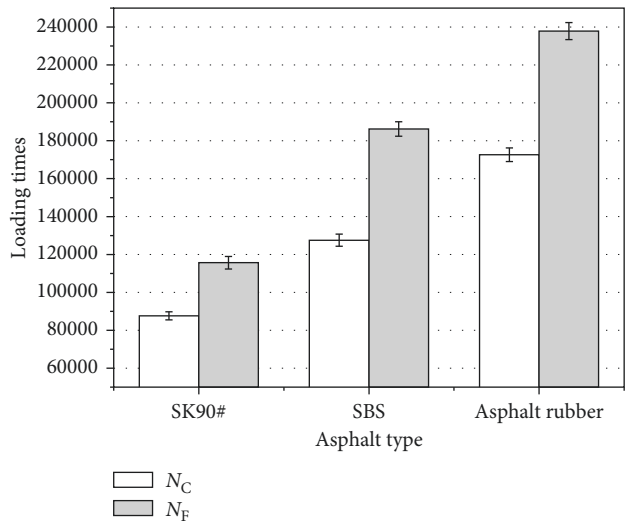

Figure 8: The influence of asphalt type on fatigue cracking life and fatigue fracture life.

The percent of embedment traditionally required for aggregate is 70% [25].

(2) Proper bonding between layers: The material composition of AR-SAMI should ensure that the asphalt overlay has sufficient shear strength in the composite structure.

Then, the optimum application rates of asphalt rubber and aggregate can be obtained by the maximum interlaminar shear strength of AR-SAMI at different temperatures.

3.2.2. Determination of Optimum Asphalt and Aggregate Application Rates for AR-SAMI. Figure 9 illustrates the interlaminar shear strength at 25°C for AR-SAMI containing different application rates of asphalt rubber and aggregate.

As shown in Figure 9, the interlaminar shear strength of AR-SAMI increases first and then decreases with the increase of aggregate application rate at one certain asphalt application rate. At several asphalt application rates, the aggregate application rate corresponding to the maximum interlaminar shear strength is 14 kg/m^2. When the aggregate application rate is fixed, the interlaminar shear strength of AR-SAMI also increases first and then decreases with the increase of asphalt application rate. The largest interlaminar shear strength was observed when the asphalt application rate was 2.2 kg/m^2 and the aggregate application rate was 14.0 kg/m^2.

The interlaminar shear strengths of AR-SAMI containing different application rates of asphalt rubber and aggregate at 45°C are shown in Figure 10.

Figure 10 shows that the interlaminar shear strength trend of AR-SAMI increases first and then decreases with the increase of asphalt application rate and aggregate application rate. The interlaminar shear strength curve gets its peak at the asphalt application rate of 2.2 kg/m^2 and the aggregate application rate of 14.0 kg/m^2.

This phenomenon is due to the lever and wedge effect. The aggregate cannot be coated completely by asphalt, and the asphalt membrane between aggregates is thin when the asphalt application rate is little. The incomplete or thin asphalt membrane cannot assure adequate adhesion between asphalt and aggregates [26], thus resulting in the interlaminar shear strength of AR-SAMI that remains at a low level. Meanwhile, too little asphalt application rate also leads to the insufficient wrapped depth of aggregates by asphalt, which will influence the waterproof effect of AR-SAMI.

But when the asphalt application rate is too large or the aggregate application rate is too low, redundant asphalt will become the lubricant which promotes the displacement of aggregates. Then, the interlaminar shear strength of AR-SAMI will decline as the asphalt application rate increases. Experience shows that too large asphalt application rate will lead to

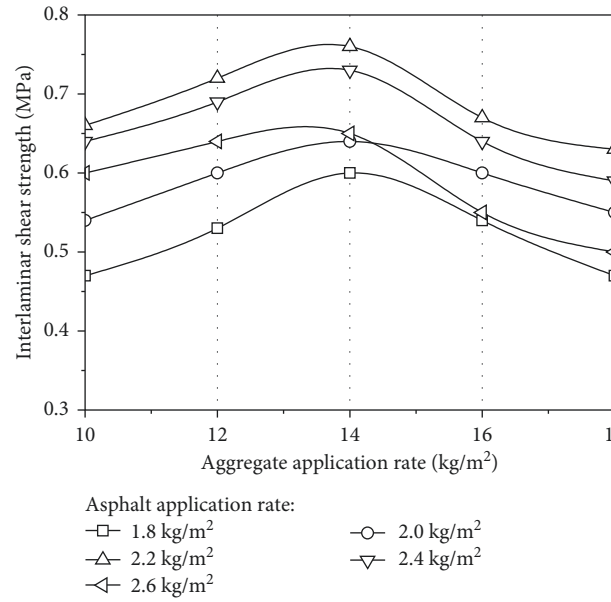

Figure 9: Interlaminar shear test results at 25°C.

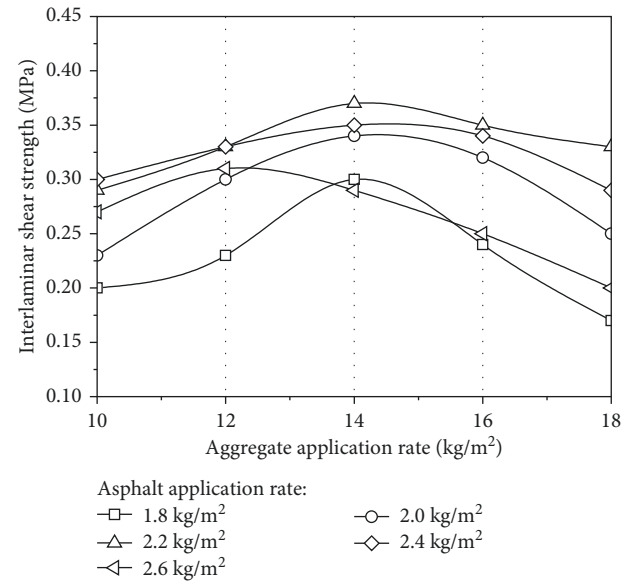

Figure 10: Interlaminar shear test results at 45°C.

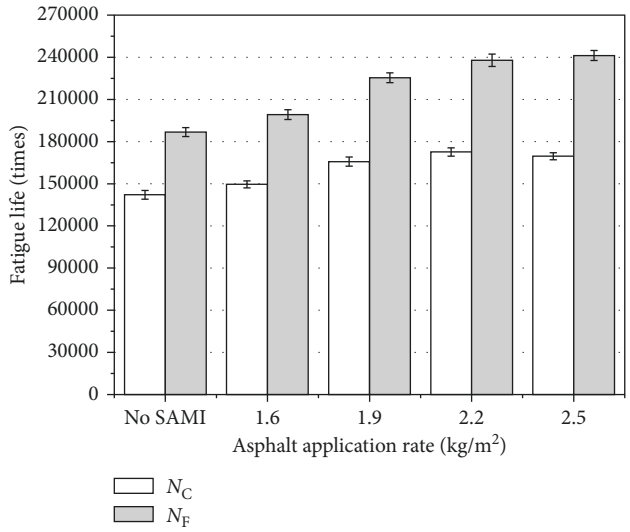

Figure 11: Fatigue cracking test results under the dry condition of 15°C.

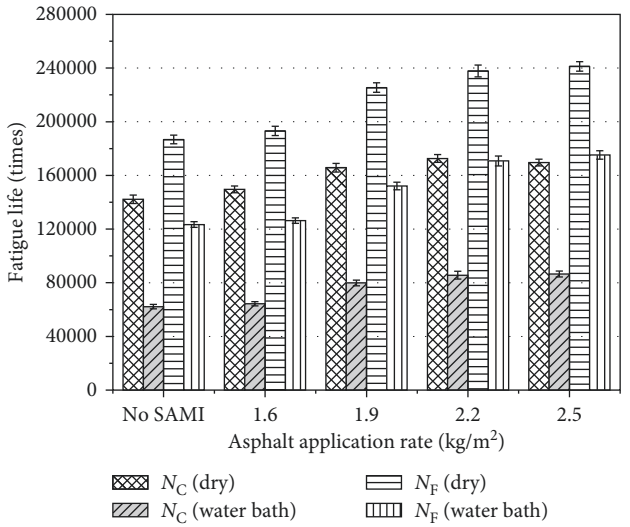

Figure 12: Fatigue cracking test results under the condition of dry and water bath at 15°C.

the bleeding and promote the formation of a weak interlayer [27]. Part of asphalt cannot be overlapped by aggregates, and sticking wheels often occur when the road roller compacts on pavement. Seriously, this phenomenon may lead to many difficulties to the construction of the pavement.

Based on these results, the asphalt application rate and aggregate application rate were determined to be 2.2 kg/m^2 and 14 kg/m^2, respectively, for AR-SAMI.

3.3. Evaluation of Anticracking Performance of AR-SAMI

3.3.1. Anticracking Effect of AR-SAMI. The fatigue cracking tests of composite beam specimens with and without AR-SAMI were carried out. The tests were conducted at the temperature of 15°C. The influence of AR-SAMI with different asphalt application rates on fatigue cracking life and fatigue fracture life is shown in Figure 11.

Figure 11 shows that the fatigue cracking life (N_C) of the asphalt layer clearly increases because of the existence of AR-SAMI when compared to the control group with no SAMI. The fatigue cracking life of the asphalt layer increases continually when the asphalt application rate increases from 1.6 kg/m^2 to 2.2 kg/m^2. After the asphalt application rate exceeds 2.2 kg/m^2, the increasing range of fatigue cracking life of the asphalt layer decreases slightly. The fatigue cracking life of the asphalt layer does not continue to increase with the increase of asphalt application rate. There is no obvious difference between the fatigue cracking life of AR-SAMI corresponding to the asphalt application rates of 2.2 kg/m^2 and 2.5 kg/m^2.

After the AR-SAMI is paved, the fatigue fracture life (N_F) of the asphalt layer also increases obviously, and the maximum increasing range reaches 29.1% approximately. The results show that fatigue fracture resistance of the composite structure improves gradually with the increase of asphalt content, but there is no significant difference between the increasing ranges of fatigue fracture life corresponding to asphalt application rates of 2.2 kg/m^2 and 2.5 kg/m^2. Based on these results, it appears that the asphalt application rate of 2.2 kg/m^2 is appropriate for AR-SAMI. This is consistent with the optimum asphalt application rate of AR-SAMI determined by the shear test.

Clearly, the AR-SAMI can not only delay the propagation of reflective cracks but also improve the ability of composite structure to resist fatigue fracture. In a certain range, the AR-SAMI has better flexibility with more asphalt rubber content. The deformation recovery ability and strain capacity of AR-SAMI with good flexibility are excellent, which will ensure longer fatigue life of composite pavement.

3.3.2. Analysis of Influence Factors on Fatigue Cracking Resistance of AR-SAMI. To analyze the influence of water and temperature on fatigue cracking resistance of AR-SAMI, the fatigue cracking tests of composite specimens with and without AR-SAMI were carried out by the Hamburg rutting instrument in a water bath condition at 15°C, 25°C, 35°C, and 45°C. The fatigue cracking life and fatigue fracture life of composite specimens under the condition of dry and water bath at 15°C are shown in Figure 12.

As shown in Figure 12, water has significant influence on the fatigue cracking life and fatigue fracture life of composite specimens. The fatigue cracking life and fatigue fracture life of composite specimens under water bath condition are lower than those under dry condition. The largest reduction of fatigue life under water bath condition is approximately 50% when compared with dry condition. The adverse effect of water on fatigue life of the pavement structure is obvious. In addition, it can also be seen from Figure 9 that when the asphalt application rate exceeds 2.2 kg/m^2, there is no improvement of fatigue life.

This phenomenon is because that the water immersion into the specimens will reduce the adhesive ability of asphalt, resulting in the decrease of overall strength of the composite specimen [28]. The free water infiltrating into the asphalt

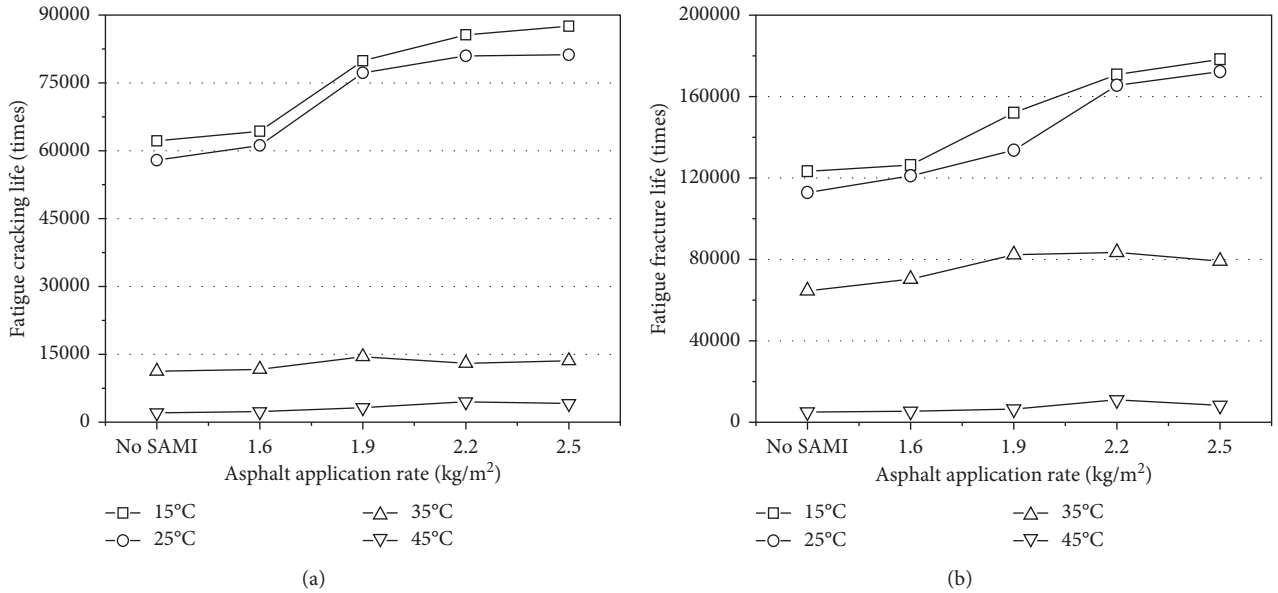

Figure 13: Fatigue cracking test results under the conditions of water bath at different temperatures: (a) fatigue cracking life; (b) fatigue fracture life.

mixture will generate hydrodynamic pressure under repeated traffic loading, which promotes the water immersion to the interface of asphalt and aggregates [29]. Then, the stripping of asphalt film from the aggregate surface or the reduction of bonding strength between asphalt and aggregate will occur under the action of vehicle loading and temperature stress [30], resulting in the deterioration of fatigue resistance of asphalt overlays. The air voids of the asphalt mixture provide the access for the infiltration of water, so they should be strictly controlled when designing the mixture for asphalt overlays [31]. The on-site air voids of the asphalt mixture should be less than 6%–8% in case of the infiltration of water [27].

The fatigue cracking life and fatigue fracture life of composite specimens with and without AR-SAMI under the conditions of water bath at 15°C, 25°C, 35°C, and 45°C are shown in Figure 13.

Figure 13 illustrates that the fatigue cracking life and fatigue fracture life increase with the increase of asphalt application rate at 15°C–25°C (room temperatures). The difference in the increasing range is not obvious when the asphalt application rate varies from 0 kg/m^2 to 1.6 kg/m^2. The fatigue cracking life and fatigue fracture life increase significantly when the asphalt application rate exceeds 1.6 kg/m^2. At 15°C, the fatigue cracking life and fatigue fracture life at the asphalt application rate of 2.2 kg/m^2 are larger by about 33% and 35%, respectively, than those at 1.6 kg/m^2. When the temperature is 25°C, the increasing range of fatigue cracking life and fatigue fracture life between different asphalt application rates is familiar with that at 15°C. With the increase of asphalt application rate, the fatigue cracking life and fatigue fracture life at 15°C–25°C do not change significantly when the rate exceeds 2.2 kg/m^2. Obviously, when the application rate of asphalt rubber is around 2.2 kg/m^2, the improved effectiveness of AR-SAMI in cracking resistance is good. This further demonstrates that the material composition design method based on the interlaminar shear strength for AR-SAMI is feasible.

The fatigue cracking life and fatigue fracture life also increase with the increase of asphalt application rate at 35°C–45°C (high temperatures), but the slope of the curve is low, namely, the growth rate of fatigue life is slow. At different asphalt application rates, the fatigue cracking life and fatigue fracture life of composite specimens in high temperature conditions decline significantly when compared with those under room temperature conditions. The effect of AR-SAMI in improving the fatigue cracking resistance of composite pavement under room temperature conditions is superior to that under high temperature conditions.

4. Conclusions

In this study, the optimization of asphalt binder for the stress-absorbing membrane interlayer (SAMI) was studied. The optimum of asphalt and aggregate application rates for AR-SAMI was also investigated by using interlaminar shear strength and fatigue cracking tests. The following conclusions may be derived based on the results obtained.

High elasticity and fatigue properties of asphalt rubber can well meet the functional requirements of SAMI. It is a good choice to select asphalt rubber as the binder for SAMI.

The application rates of asphalt and aggregate have significant influence on the interlaminar shear strength of AR-SAMI. According to the interlaminar shear strengths of AR-SAMI at room temperature (25°C) and high temperature (45°C), the optimum binder application rate of asphalt rubber and aggregate application rate for AR-SAMI are recommended as 2.2 kg/m^2 and 14 kg/m^2, respectively.

The Hamburg rutting instrument is used to load reciprocally on the composite specimen consisting of the asphalt layer, AR-SAMI, and old cement concrete. The fatigue cracking life and fatigue fracture life are monitored in the test process. According to the results, the fatigue cracking life and fatigue fracture life of asphalt overlays clearly increase after AR-SAMI is paved on the old cement concrete. Up to 30% increase in fatigue life was observed because of the use of AR-SAMI.

Water has an adverse influence on the fatigue cracking resistance of composite specimens. About 50% reduction in fatigue life was observed because of the water. The rise of temperature also presents adverse effects on the fatigue life of specimens as well. The fatigue life falls sharply when the temperature increases from 15°C–25°C to 35°C–45°C.

Data Availability

All relevant data used to support the findings of this study are included within the article. Additionally, the raw data for Figures 5–13 have been uploaded to Figshare (https://doi.org/10.6084/m9.figshare.6210074).

Conflicts of Interest

The authors declare that they have no conflicts of interest.

Acknowledgments

This study was supported by the National Natural Science Foundation of China (NSFC) (no. 51008031), Key Project of Natural Science Research of Anhui Provincial Department of Education (KJ2018A0668, KJ2017A838, and 2017jyxm0923), and Natural Science Project of College of Information Engineering (Fuyang Normal University) (no. 2017FXXZK01). The authors gratefully acknowledge their financial support.

References

[1] S. Li, X. Liu, and C. Liu, "Interlaminar shear fatigue and damage characteristics of asphalt layer for asphalt overlay on rigid pavement," *Construction and Building Materials*, vol. 68, pp. 341–347, 2014.

[2] H. Ceylan, B. J. Coree, K. Gopalakrishnan, R. Mathews, and T. Kota, *Rehabilitation of Concrete Pavements Utilizing Rubblization and Crack and Seat Methods*, IHRB Project TR-473, Center for Transportation Research and Education, Iowa State University, Ames, IA, USA, 2005.

[3] Z. Li, S. Chen, D. Zhang, H. Chen, and Y. Zhou, "Road performance of stress absorbing layers in asphalt mixture," *Journal of Chang'an University: Natural Science Edition*, vol. 28, no. 8, pp. 5–8, 2008.

[4] L. Loria, P. E. Sebaaly, and E. Y. Hajj, "Long-term performance of reflective cracking mitigation techniques in Nevada," *Transportation Research Record*, vol. 2044, no. 1, pp. 86–95, 2008.

[5] I. Gonzalez-Torre, M. A. Calzada-Perez, A. Vega-Zamanillo, and D Castro-Fresno, "Evaluation of reflective cracking in pavements using a new procedure that combine loads with different frequencies," *Construction and Building Materials*, vol. 75, pp. 368–374, 2015.

[6] D. Zamora-Barraza, M. A. Calzada-Pérez, and D. Castro-Fresno, "Evaluation of anti-reflective cracking systems using geosynthetics in the interlayer zone," *Geotextiles and Geomembranes*, vol. 29, no. 2, pp. 130–136, 2011.

[7] J. Huang, S. Chen, and Z. Li, "Advances in reflection cracking of asphalt overlay on old concrete pavement," *Materials Review A*, vol. 27, no. 2, pp. 77–80, 2013.

[8] B. J. Dempsey, "Development and performance of interlayer stress-absorbing composite in asphalt concrete overlays," *Transportation Research Record*, vol. 1809, pp. 175–183, 2002.

[9] Z. G. Ghauch and G. G. Abou-Jaoude, "Strain response of hot-mix asphalt overlays in jointed plain concrete pavements due to reflective cracking," *Computers and Structures*, vol. 124, pp. 38–46, 2013.

[10] M. Noori, O. Tataria, B. Nam, B. Golestania, and J. Greene, "A stochastic optimization approach for the selection of reflective cracking mitigation techniques," *Transportation Research Part A*, vol. 69, pp. 367–378, 2014.

[11] J. Norambuena-Contreras and I. Gonzalez-Torre, "Influence of geosynthetic type on retarding cracking in asphalt pavements," *Construction and Building Materials*, vol. 78, pp. 421–429, 2015.

[12] J. Kim and W. G. Buttlar, "Analysis of reflective crack control system involving reinforcing grid over base-isolating interlayer mixture," *Journal of Transportation Engineering*, vol. 128, no. 4, pp. 375–384, 2002.

[13] O. M. Ogundipe, N. Thom, and A. Collop, "Investigation of crack resistance potential of stress absorbing membrane interlayers (SAMIs) under traffic loading," *Construction and Building Materials*, vol. 38, pp. 658–666, 2013.

[14] O. M. Ogundipe, N. Thom, and A. Collop, "Evaluation of performance of stress-absorbing membrane interlayer (SAMI) using accelerated pavement testing," *International Journal of Pavement Engineering*, vol. 14, no. 6, pp. 569–578, 2013.

[15] Y. Tan, K. Shi, L. Li, G. Chen, and L. Ji, "Prevention of reflective cracks with high viscous asphalt stress absorbing layer," *Journal of Harbin Institute of Technology*, vol. 40, no. 2, pp. 241–245, 2008.

[16] H. Wang, Z. Dang, L. Li, and Z. You, "Analysis on fatigue crack growth laws for crumb rubber modified (CRM) asphalt mixture," *Construction and Building Materials*, vol. 47, pp. 1342–1349, 2013.

[17] S. Guo, Q. Dai, R. Si, X. Sun, and C. Lu, "Evaluation of properties and performance of rubber-modified concrete for recycling of waste scrap tire," *Journal of Cleaner Production*, vol. 148, pp. 681–689, 2017.

[18] A. M. Rodrı´guez-Alloza and J. Gallego, "Mechanical performance of asphalt rubber mixtures with warm mix asphalt additives," *Materials and Structures*, vol. 50, p. 147, 2017.

[19] H. Wang, Z. Dang, Z. You, and D. Cao, "Effect of warm mixture asphalt (WMA) additives on high failure temperature properties for crumb rubber modified (CRM) binders," *Construction and Building Materials*, vol. 35, pp. 281–288, 2012.

[20] W. G. Zhang, T. Ma, G. Xu et al., "Fatigue resistance evaluation of modified asphalt using a multiple stress creep and recovery (MSCR) test," *Applied Science-Basel*, vol. 8, no. 3, p. 417, 2018.

[21] Q. Zhou and Q. Xu, "Experimental study of waterproof membranes on concrete deck: interface adhesion under influences of critical factors," *Materials and Design*, vol. 30, no. 4, pp. 1161–1168, 2009.

[22] JTG D50-2017, *Specifications for Design of Highway Asphalt Pavement*, China Communications Press, Beijing, China, 2017.
[23] T. Gao, "Research on preventing reflection cracks of stress absorbing membranes interlayer-rubber," M.Sc. thesis, Chang'an University, Xi'an, China, 2012.
[24] Z. Zhou, Q. Zhang, and J. Zheng, "Bridge-toughening analysis of reinforcement materials preventing bituminous surface from reflection crack by FEM," *China Civil Engineering Journal*, vol. 33, no. 1, pp. 93–98, 2000.
[25] Y. Liu, "Properties research on non-continuous fiber reinforced emulsified asphalt aggregate stress absorbing layer," M. Sc. thesis, Chongqing Jiaotong University, Chongqing, China, 2013.
[26] B. Sengoz and E. Agar, "Effect of asphalt film thickness on the moisture sensitivity characteristics of hot-mix asphalt," *Building and Environment*, vol. 42, no. 10, pp. 3621–3628, 2007.
[27] Z. Zhang, *Maintenance and Rehabilitation of Expressway Asphalt Pavement*, China Communications Press, Beijing, China, 2010.
[28] G. D. Airey, A. C. Collopa, S. E. Zooroba, and R. C. Elliott, "The influence of aggregate, filler and bitumen on asphalt mixture moisture damage," *Construction and Building Materials*, vol. 22, no. 9, pp. 2015–2024, 2008.
[29] Q. Xue and L. Liu, "Hydraulic-stress coupling effects on dynamic behavior of asphalt pavement structure material," *Construction and Building Materials*, vol. 43, pp. 31–36, 2013.
[30] M. Ameri, S. Kouchaki, and H. Roshani, "Laboratory evaluation of the effect of nano-organosilane anti-stripping additive on the moisture susceptibility of HMA mixtures under freeze-thaw cycles," *Construction and Building Materials*, vol. 48, pp. 1009–1016, 2013.
[31] S. Caro, E. Masad, A. Bhasin, and D. N. Little, "Moisture susceptibility of asphalt mixtures, part 1: mechanisms," *International Journal of Pavement Engineering*, vol. 9, no. 2, pp. 81–98, 2008.